Articles

Resonance Raman Study of Halorhodopsin Photocycle Kinetics, Chromophore Structure, and Chloride-Pumping Mechanism†

James B. Ames,‡,§ Jan Raap,‖ Johan Lugtenburg,‖ and Richard A. Mathies*,‡

Department of Chemistry, University of California, Berkeley, California 94720, and Department of Chemistry, Leiden University, 2300 RA Leiden, The Netherlands

Received July 9, 1992; Revised Manuscript Received October 6, 1992

ABSTRACT: Kinetic resonance Raman spectra of the HR_{520}, HR_{640}, and HR_{578} species in the halorhodopsin photocycle are obtained using time delays ranging from 5 μs to 10 ms in 0.3 M NO_3^-, 0.3 M Cl^-, and 3 M Cl^-. The Raman intensities are converted to absolute concentrations by using a conservation of molecules constraint. The simplest kinetic scheme that satisfactorily models the data is $HR_{578} \rightarrow HR_{520} \leftrightarrow HR_{640} \rightarrow HR_{578}$. The rate constant for the $HR_{640} \rightarrow HR_{578}$ transition increases with Cl^- concentration, suggesting that Cl^- is taken up between HR_{640} and HR_{578}. The ratio of the forward to the reverse rate constants connecting HR_{520} and HR_{640} increases as the inverse of the Cl^- concentration, suggesting that Cl^- is released during the $HR_{520} \rightarrow HR_{640}$ step. The configuration about the $C_{13}{=}C_{14}$ bond of the retinal chromophore in HR_{640} is examined by regenerating the protein with [12,14-$^2H_2$]retinal. The C_{12}–^2H + C_{14}–^2H rocking vibration for HR_{640} is observed at 943 cm^{-1}, demonstrating that the chromophore is 13-cis. The changes in the resonance Raman spectrum of HR_{640} in response to ^2H_2O suspension indicates that the Schiff base linkage to the protein is protonated. None of the HR_{640} fingerprint vibrations shift significantly in ^2H_2O, suggesting that the Schiff base adopts a C=N anti configuration; this assignment is supported by the frequency of the C_{15}–^2H rocking mode (1002 cm^{-1}). The 13-cis structure for the chromophore in HR_{640} requires that thermal isomerization back to all-trans occurs in the $HR_{640} \rightarrow HR_{578}$ transition. These structural and kinetic results are incorporated into a two-state C–T model for Cl^- pumping.

Halorhodopsin (HR),[1] a retinal-containing protein found in the plasma membrane of *Halobacterium halobium*, utilizes light energy to actively transport chloride ions (Lanyi, 1986, 1988; Oesterhelt & Tittor, 1989). This chloride transport regulates the cytoplasmic ionic strength and generates a membrane potential that is used to drive ATP synthesis. Light absorption by the *all-trans*-retinal prosthetic group in HR_{578} initiates the cyclic photochemical reaction depicted in Figure 1. The initial photochemistry involves a trans → cis isomerization about the $C_{13}{=}C_{14}$ bond of the chromophore (Fodor et al., 1987). The reisomerization of the chromophore back to all-trans may occur in either the $HR_{520} \rightarrow HR_{640}$ or the $HR_{640} \rightarrow HR_{578}$ step. The molecular mechanism of Cl^- pumping in HR may be related to the mechanism of proton pumping in bacteriorhodopsin (BR), since HR and BR are structurally similar. There is ~50% homology in their amino acid sequences (Blanck & Oesterhelt, 1987; Dunn et al., 1981) and both pigments have an *all-trans*-retinal Schiff base chromophore in a similar active-site environment (Smith et al., 1984a). In addition, evidence has been presented that BR can function as a light-driven Cl^- pump under certain conditions (Der et al., 1991; Keszthelyi et al., 1990).

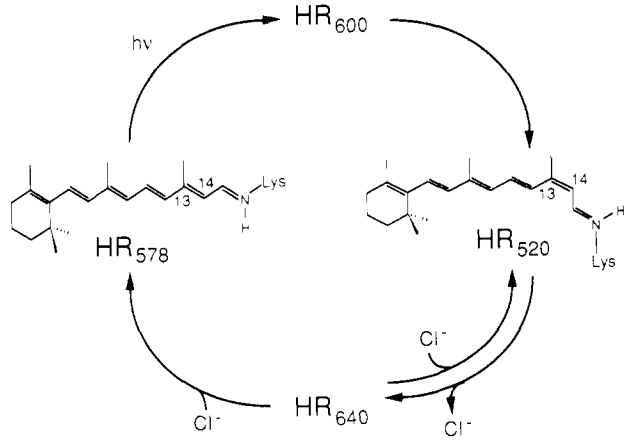

FIGURE 1: Chloride-pumping photocycle of halorhodopsin.

The photocycle kinetics of HR have been studied extensively using flash absorption techniques, and complex salt-dependent photocycle schemes have been proposed (Oesterhelt et al., 1985; Tsuda et al., 1982; Zimanyi & Lanyi, 1989). In particular, the kinetics of HR_{520} and HR_{640} depend strongly on the Cl^- concentration (Bogomolni et al., 1984). At low Cl^- concentrations or when Cl^- is replaced with NO_3^-, the HR_{640} intermediate is found at elevated concentrations while HR_{520} almost disappears (Tittor et al., 1987; Zimanyi & Lanyi, 1989). This suggests that Cl^- dissociates from the pigment during the $HR_{520} \rightarrow HR_{640}$ transition (Tittor et al., 1987; Zimanyi & Lanyi, 1989). Steady-state Cl^- currents from HR have been detected using photoelectric measurements (Bamberg

† This research was supported by a grant from the National Institutes of Health (GM 44801).

* To whom correspondence should be addressed.

‡ University of California at Berkeley.

§ Current address: Department of Cell Biology, Stanford University Medical School, Stanford, CA 94305.

‖ Leiden University.

[1] Abbreviations: HR, halorhodopsin; BR, bacteriorhodopsin; HEPES, 4-(2-hydroxyethyl)-1-piperazineethanesulfonic acid; TAPS, 3-[[tris-(hydroxymethyl)methyl]amino]propanesulfonic acid; HOOP, hydrogen out-of-plane; OG, octyl glucoside; PSB, protonated Schiff base.

0006-2960/92/0431-12546$03.00/0

et al., 1984a,b). However, direct time-resolved measurements of Cl^- release and uptake have not yet been reported. Thus, the location of the Cl^- release and uptake steps in the photocycle is unclear.

HR_{640} is a key intermediate for understanding the molecular mechanism of Cl^- pumping. It has been suggested that HR_{640} is functionally related to O_{640} in the BR photocycle, since the kinetics and λ_{max} of these intermediates are similar (Zimanyi et al., 1989). In the BR photocycle, the chromophore thermally isomerizes from cis to trans during the $N_{550} \rightarrow O_{640}$ transition (Smith et al., 1983). Does a similar chromophore isomerization occur during the formation of HR_{640}? The kinetic role of HR_{640} in the photocycle is also uncertain. HR_{640} may consist of multiple kinetic forms as suggested by phase lifetime spectroscopy (Spencer & Dewey, 1990). However, similar biphasic kinetics in the BR photocycle are best explained in terms of backreactions (Ames & Mathies, 1990; Otto et al., 1989; Parodi et al., 1984; Varo & Lanyi, 1990). To fully characterize the HR photocycle, the kinetics of the photocycle intermediates and the structure of the chromophore in HR_{640} need to be understood.

Resonance Raman spectroscopy is an effective technique for probing chromophore structure and kinetics in retinal proteins. The response of the vibrational spectra to changes in the structure of the chromophore is now well-known (Mathies et al., 1987). In addition, time-resolved resonance Raman spectroscopy is an effective probe of the kinetics of photocycle intermediates (Ames & Mathies, 1990). Previous resonance Raman studies have shown that HR_{578} contains an *all-trans*-retinal chromophore (Alshuth et al., 1985; Maeda et al., 1985; Smith et al., 1984a) and that HR_{520} contains a 13-cis chromophore (Fodor et al., 1987). Raman spectra of HR_{578} with various anions further suggest that Cl^- may interact with the Schiff base (Maeda et al., 1985; Pande et al., 1989).

We present here time-resolved resonance Raman spectra of HR_{520}, HR_{640}, and HR_{578} as a function of Cl^- activity. The HR_{640} spectrum is analyzed to determine its chromophore structure, and the kinetics of HR_{520}, HR_{640}, and HR_{578} are measured and then modeled to reveal the simplest kinetic scheme which satisfactorily describes the data. The Cl^- dependence of the microscopic rate constants suggests that Cl^- release occurs between HR_{520} and HR_{640} and that Cl^- uptake occurs between HR_{640} and HR_{578}. The reisomerization of the chromophore is shown to occur in the $HR_{640} \rightarrow HR_{578}$ transition. These observations are used to develop a C–T model for light-driven chloride ion pumping.

MATERIALS AND METHODS

Sample Preparation. Halorhodopsin from *H. halobium* strain JW-12 was isolated according to previously published procedures (Smith et al., 1984a; Taylor et al., 1983). HR membranes were solubilized with 25 mM octyl glucoside (OG). The solubilized membranes were chromatographed on a hydroxyapatite column using 25 mM OG in 3 M NaCl at pH 8.5 to wash and elute the HR. HR fractions with $A_{280}/A_{575} < 6$ were then chromatographed on a phenyl-Sepharose affinity column using 25 mM OG, 1.5 M NaCl, 50% $(NH_4)_2SO_4$, and 25 mM TAPS at pH 8.5. The affinity chromatography was repeated at least twice to fully remove all the cytochrome contamination.

Purified HR samples were dialyzed to remove the detergent because the detergent-solubilized pigment bleaches rapidly when exposed to laser excitation at room temperature. Removal of the detergent caused the HR pigment to form aggregates which were harvested by centrifugation (100000*g* for 12 h). To produce samples for Raman spectroscopy, the HR pellets were suspended in 10 mM HEPES buffer at pH 7 with either 0.3 M NaCl, 3 M NaCl, or 0.3 M $NaNO_3$.

The 12,14-$^2H_2$ and 15-^2H derivatives of retinal were synthesized according to previously published procedures (Pardoen et al., 1986). Bleaching and regeneration procedures for HR have been described (Baselt et al., 1989; Taylor et al., 1983). Typical regeneration yields ranged from 30% to 40%.

Time-Resolved Raman Spectroscopy. Raman spectra were obtained using a dual-beam flow apparatus (Mathies et al., 1987). The sample (2–3 OD/cm at 575 nm) was recirculated from a 5-mL reservoir through a 0.5- (delay times < 40 μs) or 0.8-mm diameter glass capillary at 1000 or 300 cm/s, respectively. The photocycle was initiated with a cylindrically focused 514.5-nm pump beam (0.8-mm height and 50-μm beam waist). The photoalteration parameter (Mathies et al., 1976) of the pump beam was ~1.2 using a quantum yield of 0.6 (Schneider et al., 1989) and an extinction coefficient of ~25 000 M^{-1} cm^{-1}. The depletion of HR_{578} and the formation of HR_{520} were linear in pump power up to this level. Also, the spectrum of HR_{520} under these conditions was identical to that obtained with a pump photoalteration of 0.1. To minimize photoselection artifacts in the kinetics, the polarization of the pump beam was set to 54.7° relative to that of the probe beam. Raman scattering from HR_{520} and HR_{640} was excited with 10 mW at 531 nm and 100 mW at 752 nm, respectively. In all cases, the probe beam was cylindrically focused (0.8-mm height and 50-μm beam waist) and the power was selected to produce a photoalteration parameter < 0.1, assuming a photoreaction quantum yield of unity. About 10% of the HR pigment bleached during the course of the experiment. To correct for this, probe-only spectra were taken at every delay time, and the integrated intensity for all lines between 1100 and 1700 cm^{-1} was used to correct for the loss in pigment.

Multichannel detection of the Raman scattering from HR_{520}, HR_{640}, and HR_{578} was accomplished using a cooled CCD detector (Princeton Instruments, EEV-1152) coupled to a subtractive dispersion double spectrograph with 4–7-cm^{-1} resolution. All spectra were corrected for the wavelength dependence of the spectrometer efficiency using a standard lamp. Fluorescence backgrounds were removed using a cubic spline fitting routine.

Raman spectra of HR_{520}, HR_{640}, and HR_{578} were obtained as a function of delay time (5 μs–10 ms) to measure the photocycle kinetics. The integrated Raman intensity in the spectral range 1100–1700 cm^{-1} was measured to extract the relative concentrations of HR_{520}, HR_{640}, and HR_{578} as a function of time. This analysis utilized a broad spectral region (1100–1700 cm^{-1}) instead of just the ethylenic region to permit a more constrained discrimination between each species.

Determination of Absolute Concentrations. The Raman intensities determined above are proportional to the intermediates' concentration. Without further analysis, it is impossible to relate the relative concentration of one intermediate to that of another because they were obtained using different excitation wavelengths. To resolve this problem and to obtain absolute concentrations for each kinetic species, we employ a conservation of molecules constraint (Ames & Mathies, 1990):

$$\{HR_{520}(t) + HR_{640}(t) + HR_{578}(t)\}/HR_{578}(0) = 1 \quad (1)$$

Since Raman intensity is proportional to concentration times

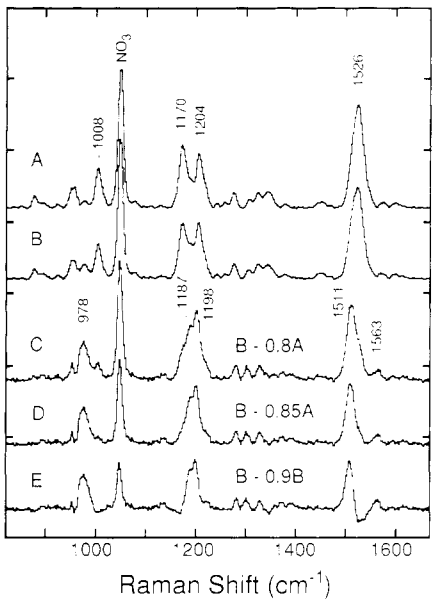

FIGURE 2: Time-resolved resonance Raman spectra of HR_{640} in 0.3 M $NaNO_3$ and 10 mM HEPES buffer at pH 7 (T = 25 °C). (A) HR_{578} probe-only spectrum excited at 752 nm. (B) Pump + probe spectrum of HR_{578} + HR_{640} produced with a 514-nm pump and 0.2-ms probe delay. (C–E) Indicated fractions of (A) are subtracted from (B) and expanded 4-fold to reveal the pure HR_{640} spectrum. The optimum subtraction coefficient is 0.85. All spectra consist of two overlapping spectral windows (700–1200 and 1150–1650 cm^{-1}) linked together at 1150 cm^{-1}.

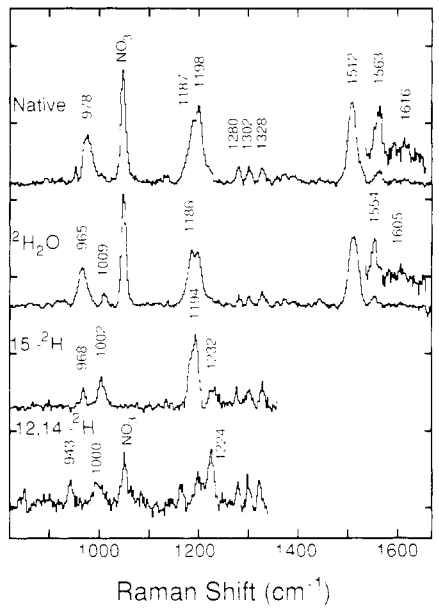

FIGURE 3: Resonance Raman spectra of native HR_{640} and its N-^2H, 15-^2H, and 12,14-$^2H_2$ derivatives. The 15-^2H and 12,14-$^2H_2$ spectra consist of just one spectral window because of sample limitations. All other conditions are the same as in Figure 2 except that 0.3 M NaCl was used instead of 0.3 M $NaNO_3$ for the 15-^2H sample.

the scattering cross section, σ, eq 1 becomes

$$\{I_{520}(t)/\sigma_{520} + I_{640}(t)/\sigma_{640} + I_{578}(t)/\sigma_{578}\}\sigma_{578} = 1 \quad (2)$$

where $I_i(t)$ is the integrated Raman intensity from intermediate i at time t normalized to that of HR_{578} at t = 0 and σ_i is the integrated scattering cross section for intermediate i. The relative cross sections (σ_i/σ_{578}) were least-squares refined to preserve conservation of molecules at all times and solvent conditions.

Kinetic Modeling. The observed concentration profiles of HR_{520}, HR_{640}, and HR_{578} were refined to a series of kinetic models. The modeling and refinement procedures have been described (Ames & Mathies, 1990).

RESULTS

Figure 2 illustrates our method for obtaining a Raman spectrum of HR_{640}. First, a probe-only spectrum of halorhodopsin (HR_{578}) is obtained using 752-nm excitation (Figure 2A). Adding a pump beam 0.2 ms upstream produces a maximal amount of HR_{640} at the probe beam position (see below). The pump + probe spectrum shown in Figure 2B probes a mixture of scattering from HR_{640} and HR_{578}. Indicated amounts of the probe-only spectrum were subtracted from the pump + probe to identify the optimal subtraction parameter for generating a pure Raman spectrum of HR_{640}. A subtraction parameter of 0.85 was chosen because it minimizes negative or positive features from HR_{578} at 1170 and 1526 cm^{-1}.

Figure 3 presents Raman spectra of HR_{640} in H_2O and ^2H_2O as well as HR_{640} regenerated with [15-^2H]- and [12,-14-$^2H_2$]retinal. In the native spectrum, the strong ethylenic line at 1512 cm^{-1} corresponds to a λ_{max} at ~640 nm (Aton et al., 1977) consistent with the λ_{max} determined from transient absorption studies (Tittor et al., 1987; Zimanyi et al., 1989). Two strong fingerprint modes are observed at 1187 and 1198 cm^{-1} which resemble the fingerprint pattern seen for the 13-cis chromophore of HR_{520} (Fodor et al., 1987) as well as for the 13-cis photocycle intermediates of bacteriorhodopsin (Mathies et al., 1987). A strong broad feature is observed at 978 cm^{-1} which may be a composite of HOOP and methyl rocking modes. A weak band is observed at 1563 cm^{-1} which shifts down to 1554 cm^{-1} in ^2H_2O. This shift supports the idea that the chromophore is linked to the protein by a protonated Schiff base group that has an exchangable hydrogen. However, the 1563-cm^{-1} frequency and the 9-cm^{-1} shift suggest that this line is a C=C mode that shifts because of its coupling with the Schiff base stretch. The insets in Figure 3 present the highest signal-to-noise spectra that we could obtain of the Schiff base region. Very faint features are observed at 1616 cm^{-1} in H_2O and 1605 cm^{-1} in ^2H_2O which might be the C=NH $(^2H)^+$ modes. The protonated Schiff base assignment is further supported by the observation of a new line at 1009 cm^{-1} in the ^2H_2O spectrum that is best assigned as a down-shifted N–^2H rocking mode.

The configuration of the C=N bond in HR_{640} can be determined by examining the coupling between the C_{14}–C_{15} stretch and N–H rocking vibrations. In chromophores having the C=N anti geometry, there is weak coupling between these vibrations so that the frequency of the C_{14}–C_{15} stretch is insensitive to deuteration of the Schiff base; however, there is strong coupling between these coordinates for molecules having the C=N syn geometry, causing the C_{14}–C_{15} stretch to shift up significantly in ^2H_2O (Smith et al., 1984b). Since none of the fingerprint modes shift significantly in ^2H_2O, this suggests that HR_{640} has a C=N anti Schiff base configuration.

To test this structural assignment, a Raman spectrum of HR_{640} labeled with [15-^2H]retinal was obtained. The frequency of the C_{15}–^2H rocking vibration is also sensitive to the C=N configuration. The C_{15}–^2H rock frequency is characteristically found in the range 970–1000 cm^{-1} for molecules having the C=N anti geometry. However, when the retinal chromophore has the C=N syn geometry, the C_{15}–^2H rock couples with the N–C_{Lys} stretch producing a characteristic mixed mode at ~1050 cm^{-1} (Ames et al., 1989; Cromwell et al., 1992). In the 15-^2H spectrum of HR_{640}, the absence of a mode at ~1050 cm^{-1} is consistent with the idea that the

chromophore in HR_{640} adopts the C=N anti geometry. Furthermore, bands are observed at 968 and 1002 cm^{-1}, which fall in the frequency range expected for the C_{15}–^2H rock of a C=N anti chromophore. The most plausible assignment is that the 1002-cm^{-1} mode is the C_{15}–^2H rock. The shift of the 978-cm^{-1} (native) mode to 968 cm^{-1} in the 15-^2H spectrum would then be due to its coupling with the C_{15}–^2H rock. The 1002-cm^{-1} frequency of the C_{15}–^2H rock in HR_{640} supports the idea that its chromophore adopts the C=N anti geometry. Finally, in the [15-^2H]HR_{640} spectrum, a line is observed at 1232 cm^{-1} which appears to have shifted up from the 1187–1198-cm^{-1} C–C stretching bands upon 15-^2H substitution. The 1232-cm^{-1} band is assigned as the C_{14}–C_{15} stretch because this mode is expected to shift up in the 15-^2H derivative (Braiman & Mathies, 1980).

The configuration about the C_{13}=C_{14} bond can be determined by examining the C_{12}–^2H + C_{14}–^2H rocking vibrations (Mathies et al., 1987). In all-trans structures, there is strong coupling between these deuterium rocks, and the C_{12}–^2H + C_{14}–^2H rock appears near 910 cm^{-1}. In the 13-cis structure, the coupling is weaker and the C_{12}–^2H + C_{14}–^2H rock combination is found at ~940 cm^{-1}. The Raman spectrum of HR_{640} labeled with [12,14-$^2H_2$]retinal displays a C_{12}–^2H + C_{14}-^2H coupled rock at 943 cm^{-1}. *This frequency demonstrates that HR_{640} contains a 13-cis-retinal Schiff base chromophore.*

Figure 4 presents Raman spectra of HR_{640} taken as a function of time in 0.3 M nitrate and 0.3 M chloride. A detailed analysis of the Raman kinetics will be presented later in the Kinetic Modeling section. Plots of the integrated Raman intensity as a function of time shows that HR_{640} rises in about 10 μs and decays on the millisecond time scale (see below). At all times the absolute concentration of HR_{640} is much lower in 0.3 M chloride than it is in 0.3 M nitrate.

Figure 5 presents our method for obtaining Raman spectra of HR_{520}. First, a probe-only spectrum of HR_{578} is obtained by using 531-nm excitation (Figure 5A). The pump + probe spectrum in Figure 5B probes a mixture of scattering from HR_{520} and HR_{578}. Figure 5C shows a spectrum of HR_{520} obtained by subtracting an optimal fraction of the probe-only spectrum from the pump + probe spectrum. This Raman spectrum of HR_{520} agrees with previously reported spectra (Diller et al., 1987; Fodor et al., 1987).

Figure 6 presents Raman spectra of HR_{520} as a function of delay time in 0.3 M nitrate, 0.3 M chloride, and 3.0 M chloride. In 0.3 M nitrate, a line is observed at 1512 cm^{-1} that is the ethylenic mode of HR_{640}. This line becomes weaker relative to the other lines in 0.3 M NaCl and completely disappears in 3 M NaCl. Plots of the HR_{520} Raman intensity as a function of time show that it decays on the millisecond time scale (Figure 7).

The Raman intensities of HR_{640}, HR_{520}, and HR_{578} at each time were converted into absolute concentrations through the conservation of molecules least-squares refinement (Ames & Mathies, 1990). This gave relative Raman cross section values (for the integrated area of the sum of all bands between 1100 and 1700 cm^{-1}) of $\sigma_{520}/\sigma_{578}$ = 1.1 at 531 nm and $\sigma_{640}/\sigma_{578}$ = 2.5 at 752 nm. Using these values, the absolute concentration of each intermediate as well as the total concentration at each time point was determined. The concentration of HR_{520}, HR_{640}, and HR_{578} as a function of time and Cl^- activity is provided in Table I, and these data are plotted in Figure 7. In 0.3 M NO_3^-, HR_{520} decays and HR_{640} rises at early times; both species are present in roughly equal concentrations beyond 20 μs, and both decay in ~3 ms to HR_{578}. In 0.3 M

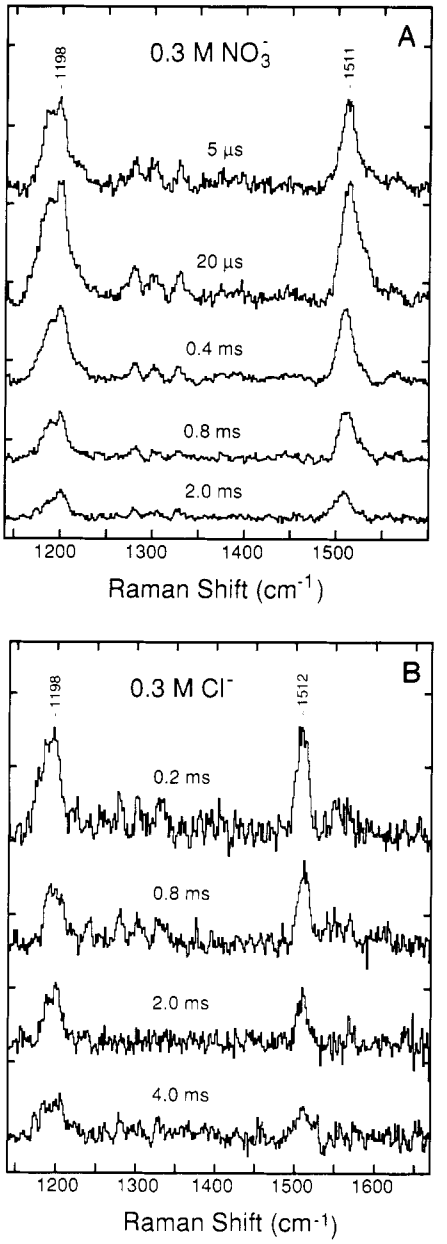

FIGURE 4: Resonance Raman spectra of HR_{640} as a function of time in 0.3 M $NaNO_3$ (A) or 0.3 M NaCl (B) at pH 7 (probed at 752 nm). All other conditions are the same as in Figure 2.

Cl^-, HR_{520} accumulates to a greater extent than HR_{640}, and both species decay in ~4 ms back to HR_{578}. Finally, in 3 M Cl^-, HR_{520} is the only photointermediate observed beyond 40 μs, and the decay of HR_{520} matches the recovery of HR_{578}.

Kinetic Modeling. A series of kinetic schemes were examined to find the simplest one that accurately describes the data. The optimal rate constants for a given kinetic scheme were determined by nonlinear least-squares refinement. Since we are fitting to absolute concentrations, microscopic rate constants are determined for the individual elementary steps in the photocycle. The simplest kinetic scheme sufficient to model all of the Raman kinetics is the sequential scheme $HR_{578} \rightarrow HR_{520} \leftrightarrow HR_{640} \rightarrow HR_{578}$. The concentrations of HR_{640} and HR_{578} were measured from 5 to 20 μs in 0.3 M NO_3^- to determine whether HR_{640} precedes or follows HR_{520}. At these early times, the HR_{640} concentration rises while HR_{578} remains constant; thus, HR_{520} must be decaying at these times. This indicates that HR_{520} preceeds HR_{640}, as has been argued from previous transient absorption work. A unidirectional sequential scheme was unable to model the parallel decay pattern

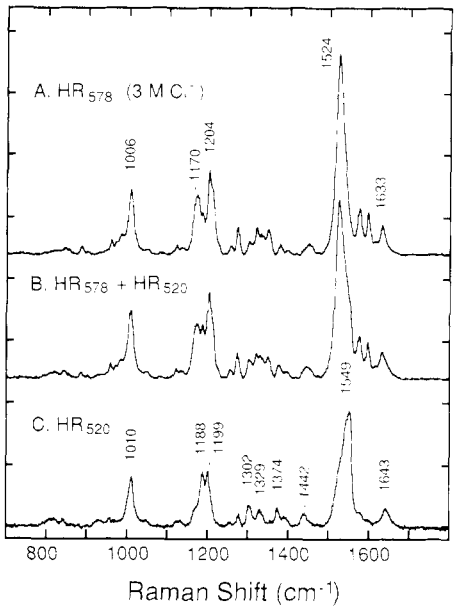

FIGURE 5: Resonance Raman spectrum of HR_{520} in 3 M NaCl and 10 mM HEPES buffer at pH 7 (T = 25 °C). (A) HR_{578} spectrum excited at 531 nm. (B) Pump + probe spectrum of HR_{578} + HR_{520} produced with a 514-nm pump and 0.2-ms delay. (C) Pure HR_{520} spectrum obtained by subtracting 75% of (A) from (B).

seen for HR_{520} and HR_{640}. A backreaction between HR_{520} and HR_{640} was necessary to simultaneously model the decay of HR_{520} and HR_{640}. A backreaction between HR_{640} and HR_{578} was not introduced because it did not improve the kinetic fits. This does not mean that the $HR_{640} \rightarrow HR_{578}$ step is irreversible. It simply means that the reverse rate constant could not be adequately determined from our data. The calculated concentrations as a function of time using the optimal kinetic scheme and rate constants are given by the solid lines in Figure 7.

The optimum rate constants for the sequential scheme are plotted as a function of Cl^- concentration in Figure 8. The figure shows that k_2 is proportional to the Cl^- concentration. This suggests that Cl^- uptake takes place between HR_{640} and HR_{578}. The Cl^- dependence for the individual values of k_1 and k_{-1} could not be determined from our data since the HR_{640} rise was only measured at one ionic strength; however, the Cl^- dependence of the ratio k_1/k_{-1} could be extracted. Figure 8 shows that k_1/k_{-1} is proportional to the inverse of the Cl^- concentration. This suggests that Cl^- is released during the $HR_{520} \rightarrow HR_{640}$ transition, in agreement with previous transient absorption analyses (Tittor et al., 1987; Zimanyi et al., 1989).

DISCUSSION

Structure of the Chromophore in HR_{640}. The determination of the retinal chromophore structure in HR_{640} is important for understanding the Cl^--pumping mechanism of halorhodopsin. Since HR_{640} kinetically and spectrally resembles the O_{640} intermediate in the BR photocycle, we wanted to determine whether HR_{640} contains an *all-trans*-retinal chromophore and whether it plays a functional role analogous to that of O_{640}.

The configuration about the C_{13}=C_{14} bond in HR_{640} was determined by regenerating HR with [12,14-$^2H_2$]retinal. The coupling between C_{12}–^2H and C_{14}–^2H rocking vibrations is strong in 13-trans chromophores, pushing the coupled deuterium rock down to ~910 cm^{-1} (Mathies et al., 1987). In 13-cis chromophores the C_{12}–^2H and C_{14}–^2H rocks are weakly

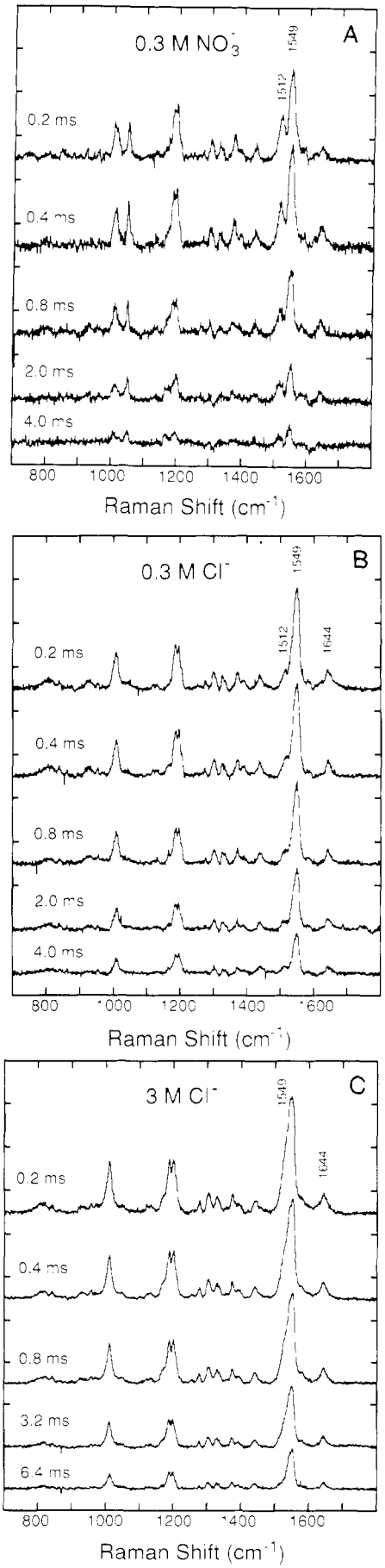

FIGURE 6: Resonance Raman spectra of HR_{520} as a function of time in (A) 0.3 M $NaNO_3$, (B) 0.3 M NaCl, and (C) 3.0 M NaCl at pH 7 (probed at 531 nm). All other conditions are the same as in Figure 5.

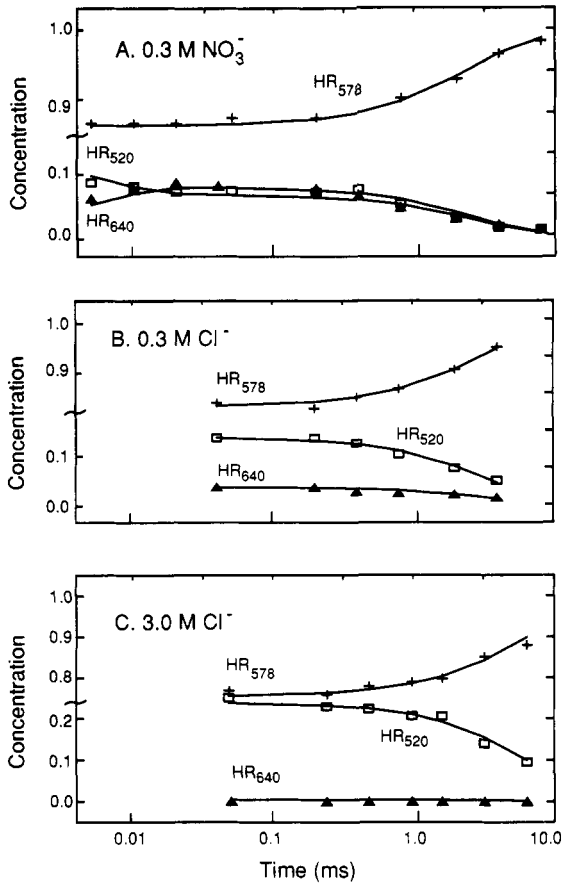

FIGURE 7: Concentration of HR_{520}, HR_{640}, and HR_{578} as a function of time in 0.3 M $NaNO_3$ (A), 0.3 M NaCl (B), and 3 M NaCl (C). The solid lines present calculated concentrations for the kinetic scheme $HR_{578} \rightarrow HR_{520} \leftrightarrow HR_{640} \rightarrow HR_{578}$ using the kinetic constants in Figure 8. The measured concentrations are represented by the discrete data points with relative errors of ±20%.

coupled, causing a higher rock frequency (~940 cm^{-1}). HR_{640} exhibits a C_{12}–^2H + C_{14}–^2H rock at 943 cm^{-1}, which is a reliable diagnostic of the 13-cis geometry.

Analysis of the fingerprint vibrations in the 15-^2H derivative provides additional support for the 13-cis structural assignment. 15-Deuteration causes the C_{14}–C_{15} stretch to shift up, producing a characteristic band at ~1230 cm^{-1} in 13-cis pigments (Braiman & Mathies, 1980). In the fingerprint region of the 15-^2H derivative of HR_{640} (Figure 3), a new band appears at 1232 cm^{-1} which is assigned as the C_{14}–C_{15} stretch. The 1232-cm^{-1} frequency of the C_{14}–C_{15} stretch further supports the 13-cis assignment.

The protonation state of the Schiff base group in HR_{640} was determined by examining the response of the vibrational spectrum to suspension in ^2H_2O buffer. A mode at 1563 cm^{-1} (and perhaps ~1616 cm^{-1}) downshifts in ^2H_2O. In addition, an N–^2H rock mode appears at 1009 cm^{-1}. These observations indicate that the chromophore in HR_{640} contains a protonated Schiff base linkage. The mode at 1563 cm^{-1} must contain substantial C=C stretching character based on group frequency arguments, while the mode at 1616 cm^{-1} is at the correct frequency to be a C=NH^+ stretch (Mathies et al., 1987; Smith et al., 1983). If the 1616-cm^{-1} mode is the C=NH^+ stretch, its low frequency and 10-cm^{-1} shift in ^2H_2O suggest that a weak Schiff base counterion interaction is responsible for the red-shifted λ_{max} of HR_{640} (Baasov et al., 1987; Fodor et al., 1989).

The configuration about the C=N bond in HR_{640} was determined by examining the sensitivity of the C_{14}–C_{15} stretch to N-deuteration. The C_{14}–C_{15} stretch is insensitive to deuteration of the Schiff base when the chromophore adopts the C=N anti geometry; however, the C_{14}–C_{15} stretch shifts up in ^2H_2O if the chromophore has a C=N syn linkage to the protein (Smith et al., 1984b). No significant shift of the fingerprint lines was observed when HR_{640} was suspended in ^2H_2O. This suggests that HR_{640} contains a C=N anti linkage between the chromophore and the protein.

To test this assignment, we determined the frequency of the C_{15}–^2H rocking vibration in HR_{640}. When the Schiff base adopts a C=N anti configuration, the C_{15}–^2H rock and N–C_{Lys} stretch are weakly coupled and the C_{15}–^2H rock mode is typically found in the range 970–1000 cm^{-1}; for molecules having the C=N syn configuration, the C_{15}–^2H rock and N–C_{Lys} stretch are strongly coupled, giving rise to a Raman active mode near 1050 cm^{-1} (Ames et al., 1989; Cromwell et al., 1992). The observation of the C_{15}–^2H rocking mode at 1002 cm^{-1} in the spectrum of the [15-^2H]HR_{640} derivative indicates that the chromophore in HR_{640} has a C=N anti Schiff base configuration.

In summary, our Raman analysis demonstrates that HR_{640} contains a 13-cis, C=N anti protonated Schiff base chromophore. Previous studies have shown that HR_{520} also contains a 13-cis chromophore (Fodor et al., 1987; Diller et al., 1987). *Therefore, the $HR_{520} \rightarrow HR_{640}$ transition does not involve a 13-cis → 13-trans isomerization. The re-isomerization back to all-trans in the HR photocycle must not occur until the decay of HR_{640}.*

HR Photocycle Kinetics. A second goal of this study was to measure and model the kinetics of the halorhodopsin photocycle. The kinetics of HR_{520}, HR_{640}, and HR_{578} were determined as a function of Cl^- activity. After conversion to absolute concentrations by using conservation of molecules, these data were adequately modeled by a sequential kinetic scheme ($HR_{578} \rightarrow HR_{520} \leftrightarrow HR_{640} \rightarrow HR_{578}$) including a backreaction between HR_{520} and HR_{640}. The rate constant connecting HR_{640} and HR_{578} increases linearly as a function of Cl^- concentration. Since the $HR_{640} \rightarrow HR_{578}$ rate constant appears pseudo-first-order with respect to Cl^- ($k_2 = k_2'[Cl^-]$), this suggests that a chloride ion is taken up by the protein in the $HR_{640} \rightarrow HR_{578}$ transition. A value of 2.3 M^{-1} ms^{-1} for k_2' satisfactorily models the data in Figure 8. Thus, the uptake of Cl^- by the protein is not diffusion limited and must involve a significant barrier. The ratio of the apparent forward and reverse rate constants (k_1/k_{-1}) for the $HR_{520} \leftrightarrow HR_{640}$ equilibrium is inversely proportional to the Cl^- concentration: $k_1/k_{-1} = k_1'/(k_{-1}[Cl^-])$. A k_1'/k_{-1}' value of 0.06 M is obtained from the data in Figure 8, which suggests that HR_{520} is intrinsically more stable than HR_{640} by ~2 kcal/mol. Since Cl^- is taken up during the backreaction, $HR_{640} \rightarrow HR_{520}$, a chloride ion must be released from the protein during the $HR_{520} \rightarrow HR_{640}$ forward step. Thus, HR_{640} is a key intermediate for mediating Cl^- transport during the photocycle.

These results are in agreement with previous transient absorption analyses which studied the Cl^- dependence of the photocycle kinetics (Oesterhelt et al., 1985; Tittor et al., 1987; Zimanyi et al., 1989). However, it should be noted that the HR_{640} rise time measured by transient absorption (Tittor et al., 1987; Zimanyi et al., 1989) is 5–10 times slower than our measurement. The difference in the HR_{640} rise kinetics might be the result of the detergent used in the absorption experiments. Detergent is known to perturb the photocycle kinetics in bacteriorhodopsin (Miercke et al., 1989). The Raman kinetics are also consistent with more complicated schemes employing parallel or branching steps; however, the

Table I: Concentration of Halorhodopsin Intermediates as a Function of Time[a]

	0.3 M NO_3^-			0.3 M Cl^-			3.0 M Cl^-		
time (ms)	HR_{520}	HR_{640}	HR_{578}	HR_{520}	HR_{640}	HR_{578}	HR_{520}	HR_{640}	HR_{578}
0.005	0.083[b]	0.067	0.85	–	–	–	–	–	–
0.01	0.078[b]	0.072	0.85	–	–	–	–	–	–
0.02	0.066[b]	0.084	0.85	–	–	–	–	–	–
0.04	–	–	–	0.12	0.031	0.86	–	–	–
0.05	0.072	0.08	0.85	–	–	–	0.25	0	0.77
0.2	0.07	0.076	0.86	0.12	0.030	0.84	0.23	0	0.75
0.4	0.08	0.064	0.85	0.11	0.025	0.86	–	–	–
0.5	–	–	–	–	–	–	0.23	0	0.78
0.8	0.05	0.039	0.89	0.09	0.021	0.88	–	–	–
1.0	–	–	–	–	–	–	0.21	0	0.79
1.6	–	–	–	–	–	–	0.20	0	0.79
2.0	0.025	0.024	0.92	0.07	0.018	0.91	–	–	–
3.2	–	–	–	–	–	–	0.14	0	0.86
4.0	0.012	0.016	0.96	0.04	0.012	0.95	–	–	–
6.4	–	–	–	–	–	–	0.10	0	0.88
8.0	0.005	0.008	0.98	0.02	0.005	0.97	–	–	–

[a] Concentration of HR intermediates obtained from time-resolved Raman spectroscopy and conservation of molecules refinement. The error for the concentrations is estimated to be ≤±20%. Relative Raman cross sections for the integrated intensity between 1100 and 1700 cm^{-1} were refined to give $\sigma_{520}/\sigma_{578} = 1.1 \pm 0.2$ at 531 nm and $\sigma_{640}/\sigma_{578} = 2.5 \pm 0.5$ at 752 nm. The solvent conditions were 10 mM HEPES at 25 °C with Cl^- or NO_3^- present as indicated. A dash indicates a time point that was not studied. [b] The HR_{520} concentrations at 5, 10, and 20 μs were calculated on the basis of conservation of molecules using the measured HR_{640} and HR_{578} concentrations at these times.

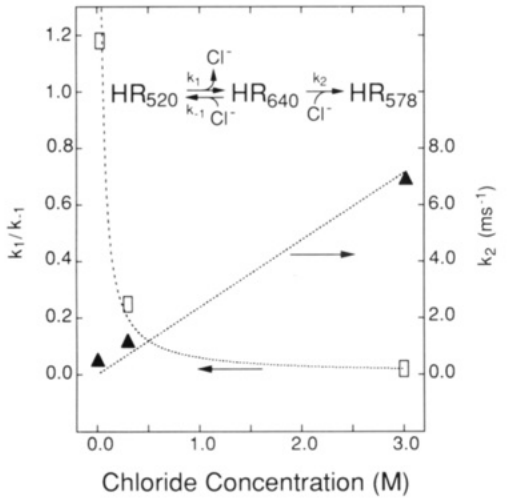

FIGURE 8: Best-fit rate constants for the halorhodopsin photocycle as a function of Cl^- concentration. Values for k_1/k_{-1} and k_2 were refined by performing a least-squares fit to the data in Table I (Figure 7) using the kinetic scheme $HR_{578} \rightarrow HR_{520} \leftrightarrow HR_{640} \rightarrow HR_{578}$. The Cl^- dependence of the rate constants was modeled by $k_1/k_{-1} = k_1'/k_{-1}'[Cl^-])$ and $k_2 = k_2'[Cl^-]$. The lines were calculated using $k_1'/k_{-1}' = 0.06$ M (dashed) and $k_2' = 2.3$ M^{-1} ms^{-1} (dotted). The rate constants are indicated by the symbols: k_1/k_{-1} (□) and k_2 (▲).

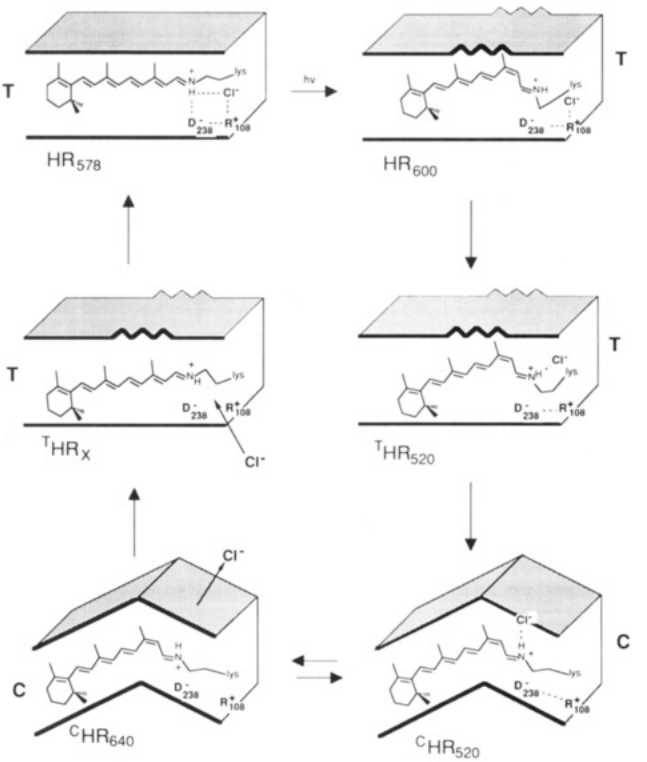

FIGURE 9: C–T model for the halorhodopsin chloride ion pump. The Schiff base, Arg-108, and Asp-238 make up the active-site chloride binding environment. A two-state protein conformational switch is used to alter the accessibility of the chloride ion binding site. In the T-state, the binding pocket sterically accommodates the 13-trans chromophore and the chloride binding site is accessible from the exterior. In the C-state, the pocket accommodates the 13-cis chromophore and the chloride binding site is accessible from the cytoplasm.

simple sequential mechanism is sufficient to model all of the data, and the microscopic steps of this scheme exhibit mechanistic significance in terms of Cl^- transport.

C–T Model for the Halorhodopsin Chloride Ion Pump. Figure 9 presents a model of the active-site structure for each HR photocycle intermediate to illustrate a molecular mechanism of Cl^- pumping. A similar mechanism has been proposed for Cl^- pumping by the acid purple form of BR and by HR (Der et al., 1991). Since HR and BR share strong similarities in their primary structure (Blanck & Oesterhelt, 1987) and protein–chromophore interactions (Fodor et al., 1987; Smith et al., 1984a; Zimanyi et al., 1989), the active-site structure for HR and BR is assumed to be similar. In BR, Asp-212 and Asp-85 interact with Arg-82 (Braiman et al., 1988; Stern et al., 1989), forming a complex counterion that stabilizes the positive Schiff base (deGroot et al., 1989). In HR, the residues corresponding to Arg-82 and Asp-212 are conserved, but Asp-85 is replaced by threonine. In our model, Cl^- plays the role of Asp-85 in the active site. The sensitivity of the Schiff base frequency in HR_{578} to the solvent anion supports this assumption (Maeda et al., 1985; Pande et al., 1989). Thus, the positive all-trans protonated Schiff base (PSB) in HR_{578} is weakly hydrogen-bonded to a complex counterion consisting of D_{238}^-, R_{108}^+, and Cl^-.

Photoisomerization to produce the primary photoproduct, HR_{600}, carries the Schiff base away from the complex

counterion, causing the chromophore absorption maximum to red-shift to ~600 nm. The photoisomerization forces the chromophore into a distorted 13-cis configuration due to steric constraints imposed by the protein. The free energy stored through steric interactions and charge separation is utilized to drive the subsequent photocycle reactions.

In the $HR_{600} \rightarrow {}^{T}HR_{520}$ transition, the active-site Cl^- moves away from R_{108}^+ and D_{238}^- to become the primary counterion for the Schiff base group, causing a blue shift in the λ_{max} to 520 nm (Baasov et al., 1987; Fodor et al., 1989). The Cl^- anion shifts in the binding pocket because of its electrostatic attraction for the positive Schiff base group. In addition, the chromophore conformationally relaxes to a planar 13-cis geometry in HR_{520} as evidenced by the lack of HOOP intensity in the resonance Raman spectrum (Diller et al., 1987; Fodor et al., 1987).

A protein conformational change is postulated to occur after the formation of ${}^{T}HR_{520}$. Large amide vibrational changes are observed in the $HR_{578} \rightarrow HR_{520}$ transition (Bousche et al., 1991). This suggests that a protein conformational change occurs when HR_{520} is formed. In the BR photocycle, a T → C protein transition has been suggested to serve as a reprotonation switch (Fodor et al., 1988; Ormos, 1991) which directs the movement of a proton from the cell exterior to the cytoplasm (Mathies et al., 1991). We propose that a similar T → C protein transition occurs in the ${}^{T}HR_{520} \rightarrow {}^{C}HR_{520}$ step. The driving force for the ${}^{T}HR_{520} \rightarrow {}^{C}HR_{520}$ transition is the reduced steric strain between the 13-cis chromophore and the protein active site. Thus, ${}^{T}HR_{520}$ may have a short lifetime and be difficult to observe. The ${}^{T}HR_{520}$ and ${}^{C}HR_{520}$ intermediates are analogous to the ${}^{T}M_{412}$ and ${}^{C}M_{412}$ intermediates in the BR photocycle (Mathies et al., 1991), so it may be possible to isolate and study them using similar techniques (Ormos, 1991). Most importantly, the ${}^{T}HR_{520} \rightarrow {}^{C}HR_{520}$ protein transition causes the Schiff base Cl^- counterion complex to move to a position/orientation in the protein that permits release of Cl^- to the cytoplasm. The T → C transition also stores free energy to be used later to drive the reisomerization of the chromophore.

Cl^- is released to the cytoplasm during the ${}^{C}HR_{520} \rightarrow {}^{C}HR_{640}$ transition as suggested by the Cl^--dependent kinetics observed here and by Zimanyi et al. (1989). The chromophore structure in HR_{640} (13-cis, C=N anti protonated Schiff base) is identical to that found in HR_{520}; however, the Schiff base counterion interaction in HR_{640} appears to be weaker. This supports the idea that Cl^- is the counterion to the Schiff base in HR_{520} and that this Cl^- counterion is released in HR_{640}.

During the $HR_{640} \rightarrow HR_{578}$ transition, Cl^- is taken up from the cell exterior, and the chromophore must isomerize back to all-trans. These two processes may occur in concert. However, it seems more reasonable that these processes occur sequentially. In BR, cis → trans isomerization and proton uptake are thought to occur sequentially (Ames & Mathies, 1990). For HR, we propose that thermal 13-cis → 13-trans isomerization occurs first, producing an intermediate denoted ${}^{T}HR_{X}$. The barrier for the cis → trans isomerization is low as a result of the extensive π-electron delocalization found in HR_{640}, evidenced by its low ethylenic stretch frequency and its red-shifted λ_{max} (Seltzer, 1987). Also, the free energy stored in the T → C transition is now utilized to drive the isomerization of the chromophore back to all-trans and make ${}^{T}HR_{X}$. The ${}^{C}HR_{640} \rightarrow {}^{T}HR_{X}$ transition is analogous to the N → O transition in BR. The isomerization during the ${}^{C}HR_{640} \rightarrow {}^{T}HR_{X}$ transition creates a Cl^- binding site which is accessible from the cell exterior. The net positive charge resulting from the protonated Schiff base, D_{238}^-, and R_{108}^+ causes Cl^- to be taken up from the cell exterior. Once Cl^- is taken up, the complex counterion is re-formed, thus completing the Cl^- pumping cycle.

CONCLUSIONS

The photocycle kinetics of halorhodopsin can be satisfactorily modeled by the kinetic scheme $HR_{578} \rightarrow HR_{520} \leftrightarrow HR_{640} \rightarrow HR_{578}$. The rate constant connecting HR_{640} and HR_{578} increases with Cl^- concentration, suggesting that Cl^- is taken up from the cell exterior during this transition. The ratio of the forward to the reverse rate constants connecting HR_{520} and HR_{640} is proportional to the inverse of the Cl^- concentration, suggesting that Cl^- is released to the cytoplasm during the $HR_{520} \rightarrow HR_{640}$ transition. On the basis of vibrational analysis of the Raman spectrum, HR_{640} contains a 13-cis, C=N anti protonated Schiff base chromophore. This shows that the reisomerization of the chromophore does not occur until the $HR_{640} \rightarrow HR_{578}$ step. Finally, we propose a mechanism for Cl^- pumping that combines two concepts. First, isomerization of the positively charged Schiff base moves the Cl^- across the binding pocket as a result of their mutual electrostatic interaction. Second, a two-state C–T protein conformational change, analogous to that proposed for BR, is used to direct the movement of the Cl^- through the protein and as an energy storage mechanism that is used to drive the reisomerization of the chromophore.

ACKNOWLEDGMENT

We thank Walther Stoeckenius and Roberto Bogomolni for supplying *H. halobium* strain JW-12 and for many valuable discussions, John Reilly and Garth Utter for assistance in preparing HR samples, and W. Thomas Pollard for writing the least-squares kinetic refinement program.

REFERENCES

Alshuth, T., Stockburger, M., Hegemann, P., & Oesterhelt, D. (1985) *FEBS Lett. 179*, 55–59.

Ames, J. B., & Mathies, R. A. (1990) *Biochemistry 29*, 7181–7190.

Ames, J. B., Fodor, S. P. A., Gebhard, R., Raap, J., van den Berg, E. M. M., Lugtenburg, J., & Mathies, R. A. (1989) *Biochemistry 28*, 3681–3687.

Aton, B., Doukas, A. G., Callender, R. H., Becher, B., & Ebrey, T. G. (1977) *Biochemistry 16*, 2995–2999.

Baasov, T., Friedman, N., & Sheves, M. (1987) *Biochemistry 26*, 3210–3217.

Bamberg, E., Hegemann, P., & Oesterhelt, D. (1984a) *Biochemistry 23*, 6216–6221.

Bamberg, E., Hegemann, P., & Oesterhelt, D. (1984b) *Biochim. Biophys. Acta 773*, 53–60.

Baselt, D. R., Fodor, S. P. A., van der Steen, R., Lugtenburg, J., Bogomolni, R. A., & Mathies, R. A. (1989) *Biophys. J. 55*, 193–196.

Blanck, A., & Oesterhelt, D. (1987) *EMBO J. 6*, 265–273.

Bogomolni, R. A., Taylor, M. E., & Stoeckenius, W. (1984) *Proc. Natl. Acad. Sci. U.S.A. 81*, 5408–5411.

Bousche, O., Spudich, E. N., Spudich, J. L., & Rothschild, K. J. (1991) *Biochemistry 30*, 5395–5400.

Braiman, M., & Mathies, R. (1980) *Biochemistry 19*, 5421–5428.

Braiman, M., & Mathies, R. (1982) *Proc. Natl. Acad. Sci. U.S.A. 79*, 403–407.

Braiman, M. S., Mogi, T., Marti, T., Stern, L. J., Khorana, H. G., & Rothschild, K. J. (1988) *Biochemistry 27*, 8516–8520.

Cromwell, M. E. M., Gebhard, R., Li, X.-Y., Batenburg, E. S., Hopman, J. C. P., Lugtenburg, J., & Mathies, R. A. (1992) *J. Am. Chem. Soc.* (in press).
deGroot, H. J. M., Harbison, G. S., Herzfeld, J., & Griffin, R. G. (1989) *Biochemistry 28*, 3346–3353.
Der, A., Szaraz, S., Toth-Boconadi, R., Tokaji, Z., Keszthelyi, L., & Stoeckenius, W. (1991) *Proc. Natl. Acad. Sci. U.S.A. 88*, 4751–4755.
Diller, R., Stockburger, M., Oesterhelt, D., & Tittor, J. (1987) *FEBS. Lett. 217*, 297–304.
Dunn, R., McCoy, J., Simsek, M., Majumdar, A., Chang, S. H., RajBhandary, U. L., & Khorana, H. G. (1981) *Proc. Natl. Acad. Sci. U.S.A. 78*, 6744–6748.
Fodor, S. P. A., Bogomolni, R. A., & Mathies, R. A. (1987) *Biochemistry 26*, 6775–6778.
Fodor, S. P. A., Ames, J. B., Gebhard, R., van den Berg, E. M. M., Stoeckenius, W., Lugtenburg, J., & Mathies, R. A. (1988) *Biochemistry 27*, 7097–7101.
Fodor, S. P. A., Gebhard, R., Lugtenburg, J., Bogomolni, R. A., & Mathies, R. A. (1989) *J. Biol. Chem. 264*, 18280–18283.
Keszthelyi, L., Szaraz, S., Der, A., & Stoeckenius, W. (1990) *Biochim. Biophys. Acta 1018*, 260–262.
Lanyi, J. K. (1986) *Annu. Rev. Biophys. Biophys. Chem. 15*, 11–28.
Lanyi, J. K. (1988) in *Transport through membranes: carriers, channels and pumps* (Pullman, A., Ed.) pp 429–440, Kluwer Academic Publishers, Boston.
Maeda, A., Ogurusu, T., & Yoshizawa, T. (1985) *Biochemistry 24*, 2517–2521.
Mathies, R., Oseroff, A. R., & Stryer, L. (1976) *Proc. Natl. Acad. Sci. U.S.A. 73*, 1–5.
Mathies, R. A., Smith, S. O., & Palings, I. (1987) in *Biological Applications of Raman Spectroscopy* (Spiro, T. G., Ed.) pp 59–108, John Wiley and Sons, Inc., New York.
Mathies, R. A., Lin, S. W., Ames, J. B., & Pollard, W. T. (1991) *Annu. Rev. Biophys. Biophys. Chem. 20*, 491–518.
Miercke, L. J. W., Ross, P. E., Stroud, R. M., & Dratz, E. A. (1989) *J. Biol. Chem. 264*, 7531–7535.
Oesterhelt, D., & Tittor, J. (1989) *Trends Biochem. Sci. 14*, 57–61.
Oesterhelt, D., Hegemann, P., & Tittor, J. (1985) *EMBO J. 4*, 2351–2356.
Ormos, P. (1991) *Proc. Natl. Acad. Sci. U.S.A. 88*, 473–477.
Otto, H., Marti, T., Holz, M., Mogi, T., Lindau, M., Khorana, H. G., & Heyn, M. P. (1989) *Proc. Natl. Acad. Sci. U.S.A. 86*, 9228–9232.
Pande, C., Lanyi, J. K., & Callender, R. H. (1989) *Biophys. J. 55*, 425–431.
Pardoen, J. A., van den Berg, E. M. M., Winkel, C., & Lugtenburg, J. (1986) *Recl. Trav. Chim. Pays-Bas 105*, 92–98.
Parodi, L. A., Lozier, R. H., Bhattacharjee, S. M., & Nagle, J. F. (1984) *Photochem. Photobiol. 40*, 501–512.
Schneider, G., Diller, R., & Stockburger, M. (1989) *Chem. Phys. 131*, 17–29.
Seltzer, S. (1987) *J. Am. Chem. Soc. 109*, 1627–1631.
Smith, S. O., Pardoen, J. A., Mulder, P. P. J., Curry, B., Lugtenburg, J., & Mathies, R. (1983) *Biochemistry 22*, 6141–6148.
Smith, S. O., Marvin, M. J., Bogomolni, R. A., & Mathies, R. A. (1984a) *J. Biol. Chem. 259*, 12326–12329.
Smith, S. O., Myers, A. B., Pardoen, J. A., Winkel, C., Mulder, P. P. J., Lugtenburg, J., & Mathies, R. (1984b) *Proc. Natl. Acad. Sci. U.S.A. 81*, 2055–2059.
Spencer, D. B., & Dewey, T. G. (1990) *Biochemistry 29*, 3140–3145.
Stern, L. J., Ahl, P. L., Marti, T., Mogi, T., Dunach, M., Berkowitz, S., Rothschild, K. J., & Khorana, H. G. (1989) *Biochemistry 28*, 10035–10042.
Taylor, M. E., Bogomolni, R. A., & Weber, H. J. (1983) *Proc. Natl. Acad. Sci. U.S.A. 80*, 6172–6176.
Tittor, J., Oesterhelt, D., Maurer, R., Desel, H., & Uhl, R. (1987) *Biophys. J. 52*, 999–1006.
Tsuda, M., Hazemoto, N., Kondo, M., Kamo, N., Kobatake, Y., & Terayama, Y. (1982) *Biochem. Biophys. Res. Commun. 108*, 970–976.
Varo, G., & Lanyi, J. K. (1990) *Biochemistry 29*, 2241–2250.
Zimanyi, L., & Lanyi, J. K. (1989) *Biochemistry 28*, 5172–5178.
Zimanyi, L., Keszthelyi, L., & Lanyi, J. K. (1989) *Biochemistry 28*, 5165–5172.

Registry No. Cl^-, 16887-00-6; NO_3^-, 14797-55-8; 13-*cis*-retinal, 472-86-6.